Simulation of PM$_{10}$ Source Apportionment at An Urban Site in Southern Taiwan by a Gaussian Trajectory Model

Chien-Lung Chen, Jeng-Lin Tsai, Feng-Chao Chung, Su-Ching Kuo, Kuo-Hsin Tseng, Pei-Hsuan Kuo, Li-Ying Hsieh, AND Ying I. Tsai

Abstract—This study applied the Gaussian trajectory transfer-coefficient model (GTx) to simulate the particulate matter concentrations and the source apportionments at Nanzih Air Quality Monitoring Station in southern Taiwan from November 2007 to February 2008. The correlation coefficient between the observed and the calculated daily PM$_{10}$ concentrations is 0.5 and the absolute bias of the PM$_{10}$ concentrations is 24%. The simulated PM$_{10}$ concentrations matched well with the observed data. Although the emission rate of PM$_{10}$ was dominated by area sources (58%), the results of source apportionments indicated that the primary sources for PM$_{10}$ at Nanzih Station were point sources (42%), area sources (20%) and then upwind boundary concentration (14%). The obvious difference of PM$_{10}$ source apportionment between episode and non-episode days was upwind boundary concentrations which contributed to 20% and 11% PM$_{10}$ sources, respectively. The gas-particle conversion of secondary aerosol and long range transport played crucial roles on the PM$_{10}$ contribution to a receptor.

Keywords—back trajectory model, particulate matter, source apportionment

I. INTRODUCTION

AIRBORNE particulate matter and gas pollutants have much effect on adverse human health, visibility degradation [1], [2] and global climate change [3], [4]. There are 72 air quality monitoring stations (AQMSs), including 57 ambient, 4 industrial, 5 traffic, 2 national park and 4 background air quality monitoring sites, measuring hourly the concentrations of sulfur dioxide, nitrite oxides, carbon monoxide, ozone, PM$_{10}$ (particulate matter aero diameter less than 10 micro meters) and volatile organic compounds in Taiwan. By analyzing the observed data of the AQMSs, the high ozone and PM$_{10}$

C.-L. Chen, Department of Industrial Engineering and Management, Fortune Institute of Technology, Kouhsiung, Taiwan (Tel: +886-7-7889888 ext 8733; fax: +886-7-7889777; e-mail: clchen@center.fotech.edu.tw).

J.-L. Tsai, K.-H. Tseng, and P.-H. Kuo, Department of Environmental Engineering, National Chung-Hsing University, Taichung, Taiwan.

F. C. Chung , (1)Department of General Education Center, Fortune Institute of Technology, Kaohsiung 831, Taiwan. and (2) Department of Applied Chemistry, Providence University, Taichung, Taiwan

L.-Y. Hsieh, Department of Chemistry, National Cheng Kung University, Tainan, Taiwan.

Su-Ching Kuo, Department of Applied Chemistry, Chia Nan University of Pharmacy and Science, Tainan, Taiwan.

Ying I. Tsai, Department of Environmental Engineering and Science, Chia Nan University of Pharmacy and Science, Tainan, Taiwan.

concentrations have long been severe air pollution issues in Taiwan. Particularly, high PM$_{10}$ episodes often occurred in winter in southern Taiwan. To develop strategies to control environmental pollutants, it is important to understand which emission sources contribute to the elevated daily PM$_{10}$ levels [5].

The purpose of this study is using a developed air quality model to estimate the source contribution to Nanzih AQMS and compare the source apportionment during PM$_{10}$ episode days with that during PM$_{10}$ non-episode days from November 2007 to February 2008.

II. METHODOLOGY

A. Air Quality Trajectory Model

The Gaussian trajectory transfer-coefficient model, GTx model, is adopted to analyze the 4-month PM$_{10}$ data at an urban site (Nanzih, Kaohsiung, Taiwan) to estimate the source apportionment of PM$_{10}$. The model describes the advection of the air parcel from a source downwind along a trajectory or from a receptor upwind along a back trajectory. The model uses the Gaussian plume equation to account for dry deposition, scavenging, upwind background pollutant transport and subsidence of pollutants from the top plenary boundary layer [6], [7]. The effects of the formation of secondary sulfate aerosol and nitrate aerosol from the oxidations of gaseous SO$_2$ and NO$_x$ emissions are also considered. For a steady-state Gaussian plume, the hourly contributed concentration C_c ($\mu g/m^3$) at a travel time t (s) and at a crosswind distance y (m) from an elevated point source with an emission rate of q_c ($\mu g/s$) of a primary pollutant c, such as primary aerosol, SO$_2$ or NO$_x$, is given as [8]:

$$C_c(t, y, z) = \frac{q_c F_c(t)}{2\pi u_s \sigma_y(t) \sigma_z(t)} \times \exp\left[-\frac{1}{2}\left(\frac{y}{\sigma_y(t)}\right)^2\right] V(t, z) \qquad (1)$$

here u_s is the effective stack height wind speed (m/s), σ_y and σ_z are horizontal and vertical dispersion parameters (m), respectively, F_c is the mass fraction of material c remaining in the plume after a travel time of t, and $V(t,z)$ is the vertical distribution fraction with respect to the plume center line. The

World Academy of Science, Engineering and Technology
International Journal of Industrial and Manufacturing Engineering
Vol:4, No:10, 2010

GTx model was tested and applied to estimate the source-receptor relationships at several locations [9]-[11].

B. Emission Inventory

The emission inventory used in this study is the Taiwan Emissions Database (TEDS), assembled by CTCI Corporation [12]. The database includes various point, line and area sources. Point sources with their emission factors and activity intensities are recorded individually. There are 9 categories for line sources and 121 categories for area sources.

Table I shows the emission inventory in the region of 30 km×30 km centered at Nanzih AQMS. It shows that SO_2 and NO_x were dominated by point sources in the region of 30 km×30 km. Especially, up to 94% of SO_2 emissions were from point sources. Most NO_x was emitted from elevated sources (67%) and then ground (line and area) sources (34%). The gas-particle conversion mechanisms of secondary aerosols from gaseous SO_2 and NO_x could contribute considerably to PM_{10}.

In addition, PM_{10} was mostly dominated by area sources (58%), then point sources (29%) and line sources (13%). The distribution of primary PM_{10} emission rate and location of the Nanzih station are shown in Fig. 1.
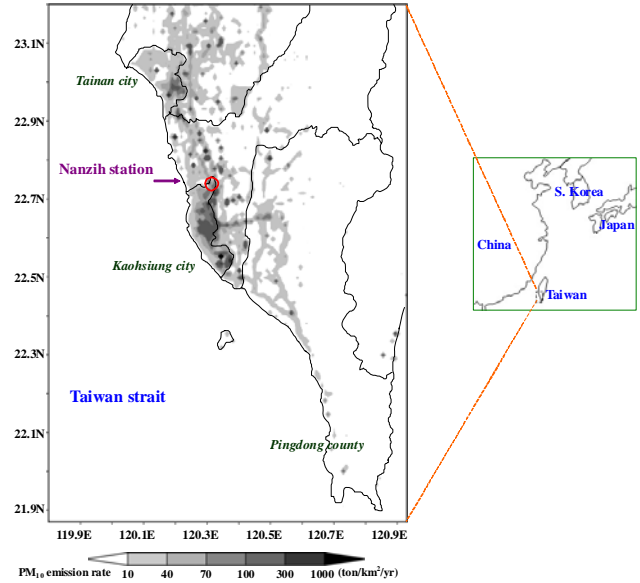
TABLE I
EMISSIONS INVENTORY IN THE REGION OF 30 KM × 30 KM CENTERED AT NANZIH STATION

Source	Emission rate (ton/year)		
	PM_{10}	SO_2	NO_x
point	6095 (28.9%)	34772 (94.4%)	40295 (67.3%)
line	2768 (13.1%)	340 (1.0%)	15379 (25.7%)
area	12251(58.0%)	1707 (4.6%)	4224 (7.0%)

C. Meteorological Data and Trajectory Line

Hourly surface wind data were obtained from Central Weather Bureau (CWB/Taiwan) and Environmental Protection Administration (EPA/Taiwan). 3-D back trajectories for 48 hours of transport arriving at the receptor site at 50m above ground level were computed from wind field data interpolated from surface meteorological stations and adjusted to the trajectory height according to a power-law profile. The temporal resolution of the observed wind data was 1 hour and the spatial resolution was about 10 km. Since the temporal and the spatial resolutions of the wind data were dense, the uncertainty of the derived trajectories was reduced [13], [14].

Fig. 1 The location of the receptor Nanzih Station (red circle), and the distribution of PM_{10} emission rate (shaded area) in southern Taiwan.

III. RESULTS AND DISCUSSION

A. Daily PM₁₀ Simulation Result

The simulated and observed concentrations of PM_{10} are shown in Fig. 2. Some daily data are not displayed due to the malfunction of PM_{10} monitoring instruments or less than 16 hourly observed concentrations available in a day in the period. The correlation coefficient and absolute bias are calculated as the performance of the GTx model. The absolute bias is defined as:

$$absolute\ bias = \frac{\left| \overline{C}_p - \overline{C}_o \right|}{\overline{C}_o} \qquad (2)$$

Where $\overline{C}_p$ is the calculated mean concentration and $\overline{C}_o$ is the observed mean concentration. Fig. 2 (a) is the time series plot for daily calculated and observed PM_{10} concentrations. There are 119 daily PM_{10} concentrations available from November 2007 to February 2008. The absolute bias of the PM_{10} concentrations for Nanzih Station receptor is 24%, and that the correlation coefficient (r) is 0.50. Fig. 2 (b) shows the observed versus calculated PM_{10} data. The dash lines indicate the calculated PM_{10} concentrations within the range of 50% underestimated or overestimated observed data. Only 11% of the absolute biases of calculated PM_{10} were greater than 50%. The simulated PM_{10} data matches well with the observed data at the receptor.

World Academy of Science, Engineering and Technology
International Journal of Industrial and Manufacturing Engineering
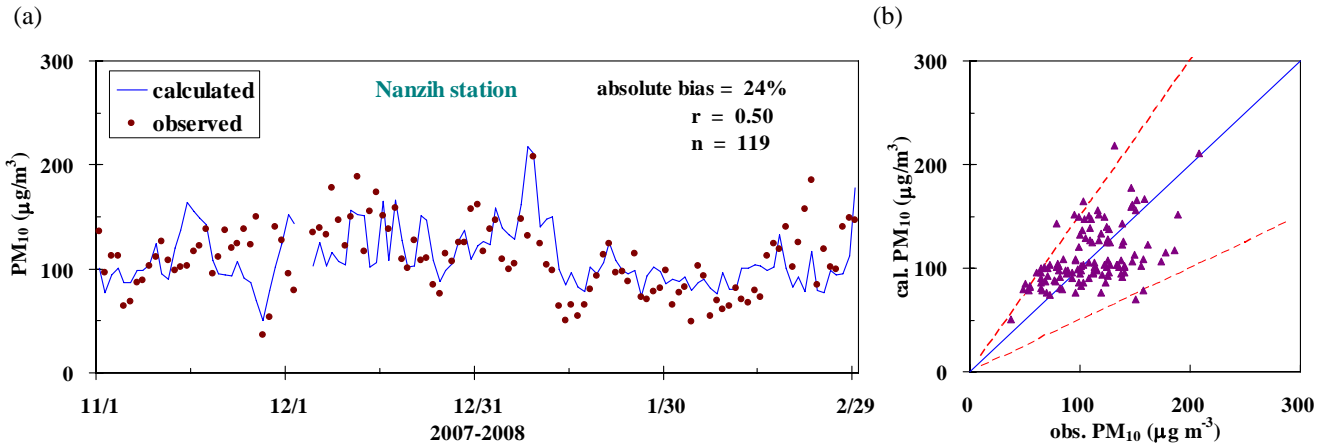Vol:4, No:10, 2010

(a)

(b)

Fig. 2 Observed and calculated PM$_{10}$ daily concentrations at Nanzih Station in Taiwan from November 2007 to February 2008.
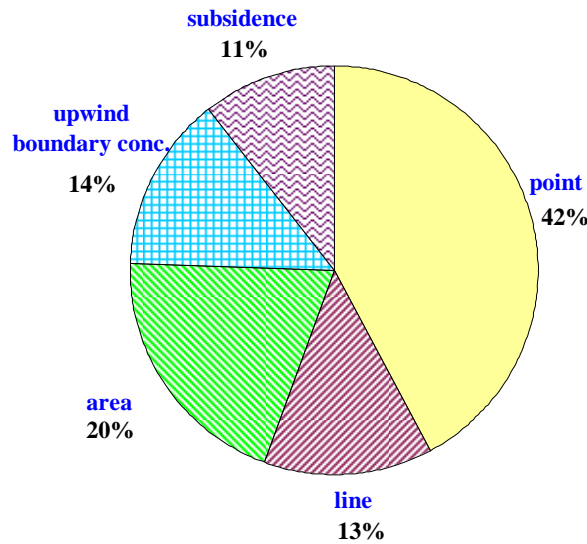(a) time series, (b) observed versus calculated data

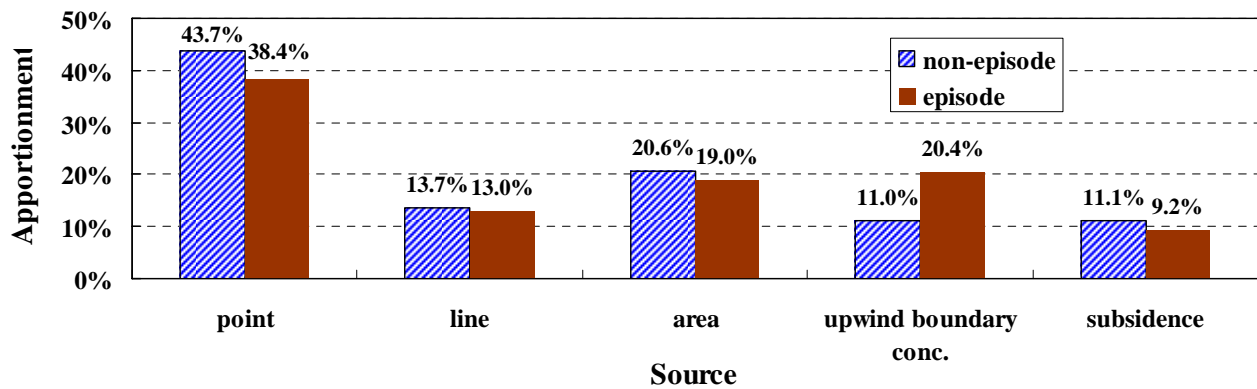Fig. 3 PM$_{10}$ source apportionment at Nanzih Station.

Fig. 4 A comparison of PM$_{10}$ source apportionment between PM$_{10}$ episode days and non-episode days at Nanzih Station.

World Academy of Science, Engineering and Technology
International Journal of Industrial and Manufacturing Engineering
Vol:4, No:10, 2010

B. Source Apportionment

At Nanzih Station, point sources were the largest PM_{10} contribution sources whereas they were only the secondary largest primary PM_{10} emission sources. Fig. 3 shows that the major sources of PM_{10} at Nanzih were point sources (42%), which emitted 29% of PM_{10} within the 30 km×30km region; area sources (20%), which emitted 58% of PM_{10} within the 30 km×30km region; and upwind boundary concentration (14%). It is evident that point sources contributed the largest fractions of PM_{10} to many of the primary PM_{10} emissions as well as SO_x/NO_x-converted aerosol.

We define that the PM_{10} episode day occurred if the daily observed PM_{10} concentration is over 130 μg/m^3. There were 31 PM_{10} episode days and 88 PM_{10} non-episode days at Nanzih Station from November 2007 to February 2008. The differences between PM_{10} source apportionment on episode days and that on non-episode days are shown in Fig. 4. The obvious difference was on the upwind boundary concentrations which contributed 20.4% PM_{10} sources on episode days and increased 9.4%, compared with that on non-episode days. The gas-particle conversion of secondary aerosol and long range transport seemed to have great influence on the downwind PM_{10} concentrations. The PM_{10} contributed fractions of the line and area sources were almost unchanged whether on episode and non-episode days. In addition, the source apportionments of the point sources and subsidence from top boundary decreased to 38.4% and 9.2% on PM_{10} episode days.

IV. CONCLUSION

In this study, the air quality trajectory model, GTx model, is adopted to analyze the 4-month PM_{10} data at an urban AQMS site to estimate the source apportionments and to compare the differences between PM_{10} on episode days and PM_{10} on non-episode days from November 2007 to February 2008. The correlation coefficient for the calculated and the observed PM_{10} concentrations is 0.50 and the absolute bias is 24%. Only 11% of the absolute biases of the calculated PM_{10} were greater than 50%. The simulated PM_{10} data matches well with the observed data at the receptor. Nevertheless, the GTx model used the simple first-order reaction rates for SO_x/NO_x gas-particle conversion mechanism. The complex photochemistry and aerosol physics and chemistry need to be improved.

In addition, The results of PM_{10} source apportionments at Nanzih station show that the major PM_{10} contribution sources are point sources (42%), area sources (20%), and then upwind boundary concentration (14%). The model results can offer the estimation for the strategy of the air quality abatement.

Finally, there were 31 PM_{10} episode days (daily PM_{10} concentration over 130 μg/m^3) and 88 PM_{10} non-episode days at Nanzih Station from November 2007 to February 2008. The obvious difference between PM_{10} source apportionment on episode days and that on non-episode days was on the upwind boundary concentrations which contributed 20.4% PM_{10} sources on episode days and increased 9.4%, compared with that on non-episode days. The gas-particle conversion of

secondary aerosol and long range transport of pollution are major contributors to downwind PM_{10} concentrations.

REFERENCES

[1] Y. I. Tsai, S.-C. Kuo, W.-J. Lee, C.-L. Chen, and P.-T. Chen, "Long-term visibility trends in one highly urbanized, one highly industrialized, and two rural areas of Taiwan," *Science of the Total Environment*, vol.382 (2-3), pp.324–341, Sep. 2007.

[2] J. Chen, Q. Ying, and M. J. Kleeman, "Source apportionment of visual impairment during the California regional PM10/PM2.5 air quality study," *Atmospheric Environment*, vol. 43, pp.6136–6144, 2009.

[3] Y. Jia, A. L. Clements, and M. P. Fraser, "Saccharide composition in atmospheric particulate matter in the southwest US and estimates of source contributions," *Journal of Aerosol Science*, vol. 41, pp.62—73, 2010.

[4] J. P. Dawson, P. N. Racherla, B. H. Lynn, P. J. Adams and S. N. Pandis, "Simulating present-day and future air quality as climate changes: Model evaluation," *Atmospheric Environment*, vol. 42, pp. 4551–4566, 2008

[5] E. Galarneau, "Source specificity and atmospheric processing of airborne PAHs: Implications for source apportionment," *Atmospheric Environment*, vol. 42, pp. 8139–8149, 2008.

[6] B. J. Tsuang, "Quantification on the source/receptor relationship of primary pollutants and secondary aerosols by a Gaussian plume trajectory model: part I – theory," *Atmospheric Environment*, vol. 37, pp.3981–3991, 2003.

[7] C.-L. Chen, B.-J. Tsuang, R.-C. Pan, C.-Y. Tu, J.-H. Liu, P.-L. Huang, H. Bai, M.-T. Cheng, "Quantification on source/receptor relationship of primary pollutants and secondary aerosols from ground sources-Part II. Model description and case study," *Atmospheric Environment*, vol. 36 , pp. 421–434, 2002.

[8] Environmental Protection Agency, United States (EPA/US), "Industrial Source Complex (ISC3) Dispersion Models—User's Guide II. Description of Model Algorithms," EPA Publication No. EPA-454/B-95-003b. US Environmental Protection Agency, Research Triangle Park, NC., 1995

[9] B. J. Tsuang, C. L. Chen, C. H. Lin, M. T. Cheng, Y. I. Tsai, C. P. Chio, R. C. Pan and P.H. Kuo, "Quantification on the source/receptor relationship of primary pollutants and secondary aerosols by a Gaussian plume trajectory model: part II. Case study," *Atmospheric Environment*, vol. 37, pp.3993–4006, 2003a.

[10] B. J. Tsuang, C. T. Lee, M. T. Cheng, N. H. Lin, Y. C. Lin, C. L. Chen, C. M. Peng and P. H. Kuo, "Quantification on the source/receptor relationship of primary pollutants and secondary aerosols by a Gaussian plume trajectory model: part III – Asian dust-storm periods," *Atmospheric Environment*, vol. 37, pp. 4007–4017, 2003b.

[11] Y. I. Tsai and C. L. Chen, "Atmospheric aerosol composition and source apportionments to aerosol in southern Taiwan," *Atmospheric Environment*, vol. 40, pp. 4751–4763, 2006.

[12] CTCI, "Update and Management for Air Pollution Emission Inventory and Estimation for Air Pollution Degradation of GNP. Report. Environmental Protection Administration, Taiwan. EPA-92-FA11-03-D039, 2003 (in Chinese).

[13] A. Stohl, "Computation, accuracy and applications of trajectories-a review and bibliography," *Atmospheric Environment*, vol. 32, pp. 947–966, 1998.

[14] P. Salvador, B. Artíñano, C. Pio, J. Afonso, M. Legrand, H. Puxbaum, S. Hammer, "Evaluation of aerosol sources at European high altitude background sites with trajectory statistical methods," *Atmospheric Environment*, vol. 44, pp. 2316–2329, 2010.